Resonant Seeding of Stimulated Brillouin Scattering by Crossing Laser Beams

H. A. Baldis,* C. Labaune, E. Schifano, N. Renard, and A. Michard

Laboratoire pour l'Utilisation des Lasers Intenses, Centre National de la Recherche Scientifique, Ecole Polytechnique, 91128 Palaiseau Cedex, France

(Received 20 March 1996)

This Letter presents the first experimental evidence of seeding of ion acoustic waves (IAW) from stimulated Brillouin scattering along the resonant direction between two interaction beams. Using a secondary interaction beam at a reduced intensity acting as seed, a well defined resonance was observed along the bisecting direction between the two laser beams. A strong reduction of the IAW was observed along off-resonance directions, including for backscatter of the primary beam. [S0031-9007(96)01305-1]

PACS numbers: 52.35.Nx, 52.35.Fp, 52.40.Nk, 52.50.Jm

An issue of critical importance in inertial confinement fusion (ICF) is the characterization and control of stimulated Brillouin scattering (SBS). The large size plasma encountered in *Hohlraums* can produce levels of scattered light that reduces the energy coupling, as well as modifies the light distribution, affecting the symmetry of capsule implosion [1]. The study of SBS is further complicated by the simultaneous crossing of interaction beams, which takes place near the laser entrance hole (LEH) of a *Hohlraum*. SBS driven by different beams can interact with each other, mutually modifying their behavior. This effect not only modifies light distribution, but adds to the complexity of the physics of the interaction and to the difficulty in analyzing experimental results.

We present in this Letter the first experimental demonstration of modification of SBS driven by one interaction beam, in the presence of a secondary beam, acting as a seed beam. These results include the first observation of resonant behavior when ion acoustic waves (IAW) driven by two different beams have a common wave vector, and the first evidence that overlapping beams can have a detrimental effect to the growth of SBS, in situations where there is a mismatch between IAW from two independent SBS decay processes. Since the purpose of the present study is the influence of crossing laser beams to the growth of SBS, the secondary beam was kept at a lower intensity arriving 200 ps ahead of the primary beam, to act only as a seed beam.

Stimulated Brillouin scattering consists of the decay of the incident electromagnetic (EM) wave $(\omega_0, \mathbf{k}_0)$ into a scattered EM wave $(\omega_{\rm SBS}, \mathbf{k}_{\rm SBS})$ and an IAW $(\omega_{\rm IAW}, \mathbf{k}_{\rm IAW})$, where ω and $\mathbf{k}$ are the respective frequency and wave vector for each wave [2,3]. The study was performed using Thomson scattering to measure the IAW associated with SBS, using a short wavelength probe beam. This technique provides the most direct characterization of the waves, including their frequency, wave vector, and location [4]. Wave-vector resolution permitted us to observe the effect of the seed beam along different directions within the interaction region.

The problem of crossing laser beams has been addressed in the context of energy transfer between beams. Recent theoretical works show that energy transfer can take place through a parametric process, such as forward stimulated Brillouin scattering, either in the case of illumination with multiple frequencies [5] or by frequency beating between beams with the same frequency [6]. As will be discussed later, neither of these works apply to the present results. The effect of overlapping laser beams on parametric instabilities has been studied analytically by DuBois *et al.* [7] and by Pesme *et al.* [8]. These studies addressed the situation where a large number of beams of equal intensity overlap in a symmetrically distributed conical geometry.

The experimental configuration was the following. The primary interaction beam arrived normal to the preformed plasma, with the seed beam incident at an angle of 22.5° with respect to the primary beam. The 600 ps FWHM Gaussian beams were all in the same plane and arrived at the target in the following sequence: $t = 0$, 1.48, 1.52, 1.72 ns for plasma producing, Thomson probe, seed and pump beams, respectively. The interaction beams were focused with $f/6$ lenses through random phase plates (RPP) of 2 mm square elements. The resulting focal spot diameter was 320 μm FWHM, with focal depths of 1.5 mm. The maximum average intensity in the focal spot was $I_{\rm pump} = 10^{14}$ W/cm^2.

The Thomson scattering probe was focused with a combination of lens and RPP with elongated elements, to form a focal region 100 μm by 1 mm along the axis of the interaction beam, allowing to image the location of the waves over the whole interaction region. The probe beam, with aperture $f/3$, was incident at an angle of 72° with respect to the interaction axis, and scattered light was collected with angles between 11° and 47° from the probe axis. Other diagnostics included time resolved wavelength spectrum of IAW by Thomson scattering, and time resolved spectra of the SBS light, along the direction of backscatter for the primary beam. Thomson scattered light was collected with a parabolic mirror and imaged onto streak

0031-9007/96/77(14)/2957(4)$10.00

cameras and spectrometers with secondary spherical mirrors. The parabolic mirror was large enough to collect scattering light from a large range of IAW, using the same probe beam. The targets were 450 μm diameter, 1.5 μm thick, $(CH)_n$ disks. The plasma has been well characterized over many experimental campaigns [9,10]. The electron density at the peak of the plasma profile evolved from $0.25n_c$ to $0.08n_c$, from the beginning to the end of the interaction beam (where $n_c = 1.1 \times 10^{21}$ cm^{-3} is the critical electron density for $\lambda_0 = 1.05$ μm light). The density profile has a quasi-inverse-parabolic form along the interaction axis, with a FWHM of 1 mm. The electron temperature (T_e) of the plasma, obtained by Thomson scattering in the absence of the interaction beam, was between 0.4 and 0.5 keV.

The best way to describe the results of this experiment is in terms of a polar diagram for the IAW associated with each laser beam. The angular plot of wave vectors of IAW associated with SBS for all scattering directions is shown in Fig. 1(a) for one laser beam. The polar diagram gives the magnitude of $\mathbf{k}_{\mathrm{IAW}}$ for each direction θ_{IAW} of the IAW, where $\theta_{\mathrm{IAW}} = (\theta_{\mathrm{SBS}} - 180°)/2$, and θ_{SBS} is the scattering angle of the EM wave with $k_{\mathrm{SBS}} \approx k_0$. We will base the discussion on the directions of the IAW and not on the SBS scattering angle itself. If we superimpose the $\mathbf{k}_{\mathrm{IAW}}$ polar diagrams for two interaction beams, the overlap of the two circles gives, as a function of angle, the relative magnitude for the two $\mathbf{k}_{\mathrm{IAW}}$ and the associated mismatch between waves. This is shown in Fig. 1(b) for the angle of 22.5° between the interaction beams. The shaded area in Fig. 1(b) shows the direction where the wave vectors for the IAW driven by each interaction beam have the same magnitude and direction. This particular direction along the bisector between the two beams will be referred to as the resonance direction. The Thomson scattering k vectors are shown in Fig. 1(c).

Ion acoustic waves traveling along different directions were recorded with temporal and spatial resolution. The selected IAW directions correspond to the backscatter directions for each of the two beams [see Fig. 1(b)], as well as for intermediate directions. The direction of observation was defined by masks on the Thomson scattering optics, limiting the collection angle to 5°, and in steps of 5°. Figure 2 shows the temporal evolution of space resolved IAW for two different directions of IAW: Fig. 2(a) along the direction of resonance indicated by the shaded area in Fig. 1(b), and Fig. 2(b) along the direction of backscatter for the pump beam. Different frames correspond to various reduced intensities of the seed beam, keeping the intensity of the pump beam constant at $I_{\mathrm{pump}} = 10^{14}$ W/cm^2. In Fig. 2(a) there are two signals in time, which correspond, respectively, to the IAW and to electron plasma waves (EPW) driven by stimulated Raman scattering (SRS). Scattered light from EPW has been collected on the same streak camera as IAW, using the multiple slit technique [11] and a different set of color filters than IAW. The relative intensity between the IAW and EPW waves shown in Fig. 2(a) is arbitrary, and depends on the relative attenuations used on the camera.

Frame 1 in Fig. 2(a) shows the evolution of waves along the direction of resonance in the absence of seed beam ($I_{\mathrm{seed}} = 0$). The second frame in Fig. 2(a) shows the IAW in the presence of the seed beam, at an intensity of $I_{\mathrm{seed}} \approx 10^{13}$ W/cm^2, that corresponds to $I_{\mathrm{seed}}/I_{\mathrm{pump}} \approx 10\%$. Enhancement of IAW is clearly observed. The level and duration of IAW are further modified by increasing the seed beam intensity to $I_{\mathrm{seed}} = 3 \times 10^{13}$ W/cm^2 ($I_{\mathrm{seed}}/I_{\mathrm{pump}} \approx 30\%$), as shown in the third frame of the same figure. All three frames were obtained with the same attenuation on the camera. The total signals, integrated in time and space, are plotted in Fig. 3(a), as a function of the seed-beam intensity.

An important and unexpected result was obtained when probing along off-resonance directions. Figure 2(b) shows space and time resolved IAW, similar to Fig. 2(a), but along the direction of backscatter for the pump beam. For the shots in Fig. 2(b), only IAW signals are displayed. The relative intensities of IAW between the first frame in Fig. 2(a) and Fig. 2(b) are almost the same, but using different attenuations in front of the camera. Even for small levels of seed beam ($I_{\mathrm{seed}} = 10^{13}$ W/cm^2), a strong reduction was observed on the level of IAW, as shown in the second frame of Fig. 2(b). Further reduction was obtained as the intensity of the seed beam was increased, with a total reduction of a factor of 8 at $I_{\mathrm{seed}} = 3 \times 10^{13}$ W/cm^2. Figure 3(b) shows the intensities of scattered light from IAW for this off-resonance direction, integrated in time and space as a function of seed-beam intensity, showing the drastic effect on the IAW even at low seed-beam intensities. A ratio of $I_{\mathrm{seed}}/I_{\mathrm{pump}} = 3\%$ is sufficient to reduce the total observed level of scattered light from IAW by a factor of 5.

Reduction on the level of scattered light from IAW was observed at either side off the direction of resonance. Figure 4 shows levels of IAW for five different directions in increments of 5°, as a function of seed-beam intensity. Signals have been normalized to 1 in the absence of seed beam. The maximum increase corresponds to the

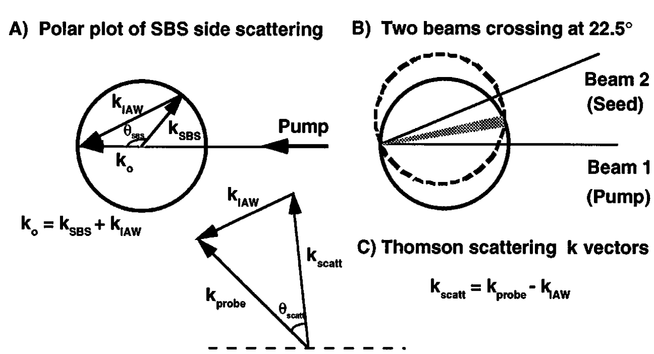

FIG. 1. Polar plot of ion acoustic waves of SBS for all scattering angles (a) and for the combination of two interaction beams separated by 22.5° (b), and Thomson scattered k vectors (c).

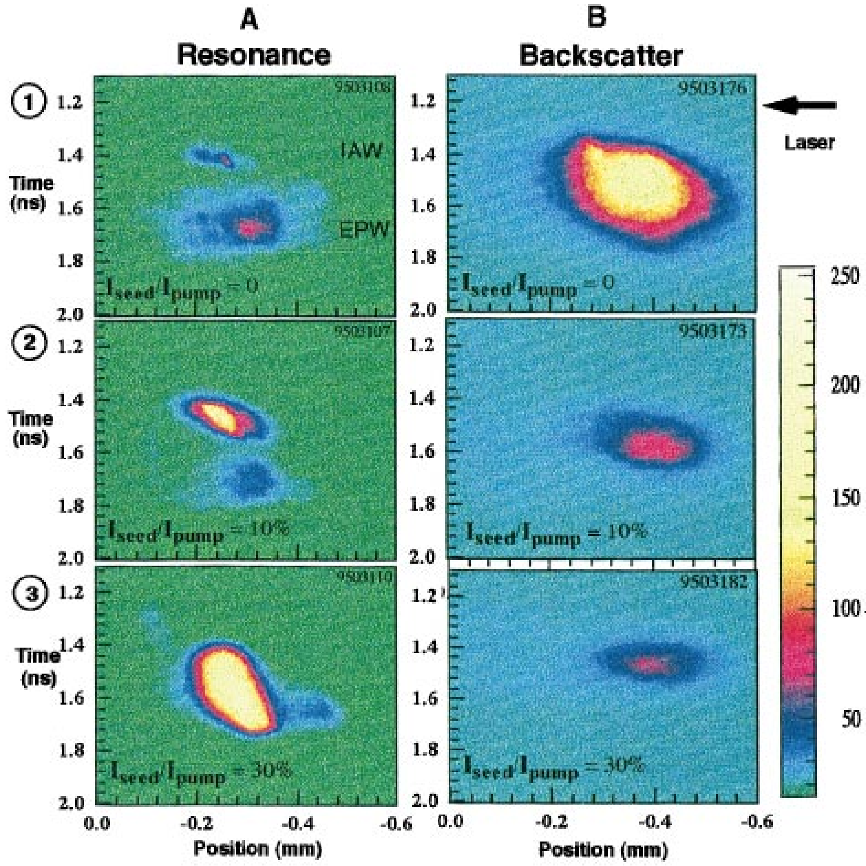

FIG. 2(color). Temporally resolved location of ion acoustic waves, along the direction of resonance (a), and along the direction of backscatter for the pump beam (b). The interaction beam arrives from the right, and the summit of the plasma is at position $z = 0$. The time scaled is referred to $t = 0$ for the peak of the plasma forming beam. The seed beam to pump beam intensity ratio $I_{\mathrm{seed}}/I_{\mathrm{pump}}$ is as follows for the different frames: (1) 0, (2) 10%, and (3) 30%.

resonance direction, and shows the dramatic effect of the seed beam on the IAW. It is important to notice the narrow angle within which the enhancement takes place. At 5° away from resonance, the mismatch in wave vector between the seed and pump beams is sufficient to change a strong enhancement into a strong reduction in the level of IAW. For a low seed-beam intensity ($I_{\mathrm{seed}}/I_{\mathrm{pump}} = 3\%$), the amount of reduction off resonance is a much larger effect than the enhancement at resonance.

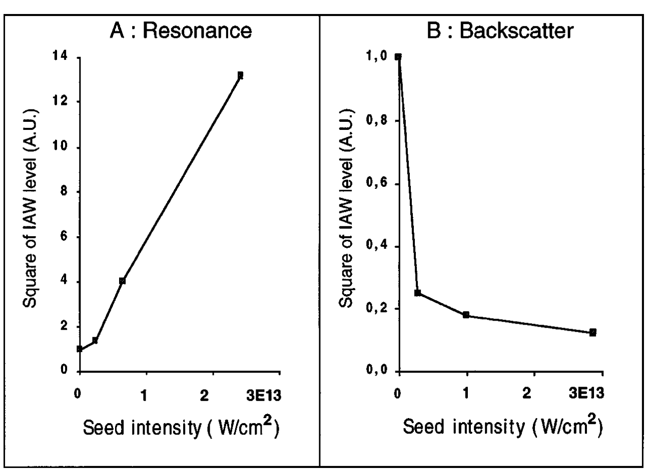

FIG. 3. Levels of intensities of Thomson scattered light from ion acoustic waves as a function of seed beam intensity, integrated in time and space, for the same shots of Fig. 2.

In their study of the effect of overlapping laser beams on parametric instabilities, DuBois *et al.* [7] find that for many overlapping beams ($N \geq 2$), the threshold for collective SBS is decreased, with respect to a single beam SBS, by a factor proportional to the number of beams, with the lowest threshold for collective SBS modes sharing a common daugther wave along the symmetry axis. Although this analysis does not apply exactly to our conditions, where modifications to the IAW is observed by only adding a second beam and at a much reduced intensity, we observe that the ion acoustic waves are preferential along the symmetry axis.

Recent work on crossing laser beams has addressed the problem of energy exchange between beams [5,6]. Although in both of these papers energy transfer takes place through coupling by an SBS process, neither case applies to the present experiment. In the work of Kruer *et al.* [5], coupling between beams takes place when using multicolor beam smoothing [12], with frequency difference between colors resonant with SBS, thus seeding the instability. In the work of Eliseev *et al.* [6], two crossing beams with the same frequency produces an

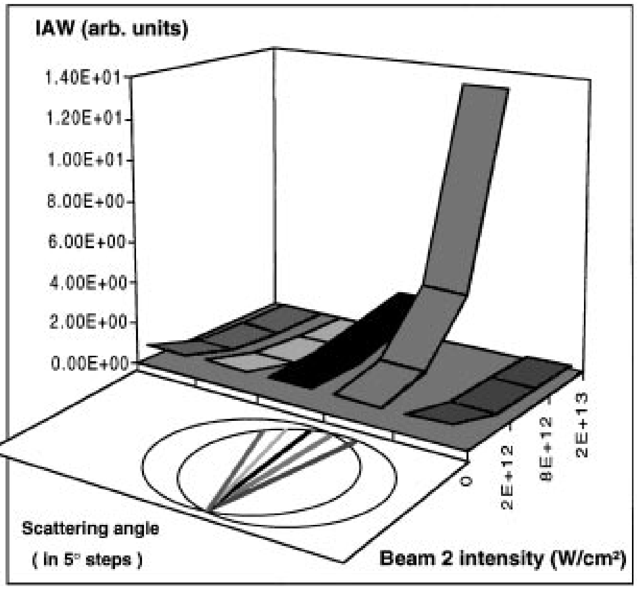

FIG. 4. Combined plot of the modified levels of ion acoustic waves from SBS for different directions, as a function of seed-beam intensity. Signals are normalized to 1 for $I_{\text{seed}} = 0$. The green line corresponds to the direction of resonance. The angular bandpass for each direction is 5°, in steps of 5°.

interference pattern that enhances forward SBS, resulting in a time dependent energy exchange between the beams.

The IAW enhancement observed along the resonant direction is clear evidence of the importance of the initial noise level from which SBS grows. At the onset of the pump beam, the instability starts to grow from ion fluctuations driven by the seed beam, having the right wave vector, rather than from thermal fluctuations. The effect is significant, even if the average intensity of the seed beam is relatively low. Since enhancement is observed over a very narrow range of angles, the allowable mismatch between the wave numbers of seed and pump IAWs has to be small. As shown in Fig. 4, the resonance is limited to an angle of approximately 5°, thus limiting the mismatch to $\Delta k_{\text{IAW}}/k_{\text{IAW}} \approx 1\%$. The observed enhancement is not an outcome of increased laser intensity; laser shots done with a single (pump) beam at higher intensities (such as $I_{\text{pump}} + I_{\text{seed}}$) have not shown such enhancement. Given the low intensity of the seed beam, it is unlikely that the observed enhancement is due to a modification of the collective growth rate [7].

The reduction of IAW off resonance is more difficult to explain. This is the first evidence that levels of IAW from SBS can be reduced as a consequence of introducing a second interaction beam. It is clear from Fig. 3(b) that small levels of seed beam can significantly reduce the growth of SBS driven by the primary beam. A possible explanation for this effect is the presence of IAW driven by the seed beam, in either backscatter or sidescatter, which are seen by the pump beam as long wavelength ion waves. It has been observed in numerical simulations [13] that long wavelength ion fluctuations produce a nonlinear inhibition of SBS by introducing an additional damping for the resonant IAW. The evolution of IAW has been studied by Cohen *et al.* [14] using 2D hybrid code simulations, to allow for sidescattering to interact with backscattered SBS. Their results show that IAW driven by backscatter SBS (a 1D phenomena) saturate and relax by 2D effects such as sideways scattering, concurrent with the generation of long wavelength modes.

The results presented here show the sensitivity of a parametric instability, such as SBS, to the initial conditions at the point of departure. A detailed characterization of the ion fluctuations and turbulence is essential, besides the plasma conditions, if we are going to attempt to model the overall evolution of an instability.

The authors acknowledge the support of the technical groups of LULI that made this work possible.

*Also at Lawrence Livermore National Laboratory, Livermore, CA 94550.

[1] J. Lindl, Phys. Plasmas **2**, 3933 (1995).
[2] H. A. Baldis, E. M. Campbell, and W. L. Kruer, in *Physics of Laser Plasma,* edited by A. Rubenchik and W. Witkowski (North-Holland, Amsterdam, 1991), pp. 361–434.
[3] W. L. Kruer, *The Physics of Laser Plasma Interactions* (Addison-Wesley Publishing Company, Inc., Redwood City, CA, 1988).
[4] D. M. Villeneuve, H. A. Baldis, and J. Bernard, Phys. Rev. Lett. **59**, 1585 (1987).
[5] W. L. Kruer, S. C. Wilks, B. B. Afeyan, and R. K. Kirkwood, Phys. Plasmas **3**, 1 (1996).
[6] V. V. Eliseev, W. Rozmus, V. T. Tikhonchuk, and C. E. Capjack, Phys. Plasmas **3**, 2215 (1996).
[7] D. F. DuBois, B. Bezzerides, and H. A. Rose, Phys. Fluids B **4**, 241 (1992).
[8] D. Pesme, R. L. Berger, E. A. Williams, A. Bourdier, and A. Bortuggo-Lesne, Phys. Rep. (to be published).
[9] C. Labaune, H. A. Baldis, N. Renard, *et al.,* Rapport Scientifique du Laboratoire pour l'Utilisation des Laser Intenses **A4–A6** (1993).
[10] C. Labaune, H. A. Baldis, N. Renard, E. Schifano, S. Baton, A. Michard, W. Seka, R. E. Bahr, B. Bauer, K. Baker, and K. Estabrook, Phys. Rev. Lett. **75**, 248 (1995).
[11] H. A. Baldis and C. Labaune, Rev. Sci. Instrum. **67**, 451 (1996).
[12] D. Eimerl (private communication).
[13] A. Maximov, W. Rozmus, V. T. Tikhonchuk, D. F. DuBois, and H. A. Rose, Phys. Plasmas **3**, 1689 (1996).
[14] B. I. Cohen, B. F. Lasinski, A. B. Langdon, and E. A. Williams, in *Invited and Review Papers of the 37th Annual Meeting of the Division of Plasma Physics of the American Physical Society, Louisville, 1995* (AIP, Woodbury, NY, 1996).